Natural Frequency Analysis of a Porous Functionally Graded Shaft System

Arnab Bose, Prabhakar Sathujoda

Abstract—The vibration characteristics of a functionally graded (FG) rotor model having porosities and micro-voids is investigated using three-dimensional finite element analysis. The FG shaft is mounted with a steel disc located at the midspan. The shaft ends are supported on isotropic bearings. The FG material is composed of a metallic (stainless-steel) and ceramic phase (zirconium oxide) as its constituent phases. The layer wise material property variation is governed by power law. Material property equations are developed for the porosity modelling. Python code is developed to assign the material properties to each layer including the effect of porosities. ANSYS commercial software is used to extract the natural frequencies and whirl frequencies for the FG shaft system. The obtained results show the influence of porosity volume fraction and power-law index, on the vibration characteristics of the ceramic-based FG shaft system.

Keywords—Finite element method, functionally graded material, porosity volume fraction, power law.

I. INTRODUCTION

THE Functionally Graded Material (FGM) is a relatively new class of inhomogeneous advanced material in the spectrum of engineering composites. A typical FGM is composed of ceramic and metal whose volume fractions are varied along the layers. The volume fractions and the material properties of each layer of an FGM are varied smoothly along the desired direction based on several material laws such as power law, exponential law, sigmoid law etc. The development of FGMs mitigated the problems of delamination, debonding and residual stresses found in traditional composites at higher temperature Due to their ability to withstand high temperatures and reduced weight, FGMs are being used as a replacement for traditional materials in aerospace, automobiles, biomedical, opto-electronics and several other segments. However, the manufacturing techniques of FGMs such as powder metallurgy involve specific control of temperatures. Often micro-voids and porosities develop in the layers during sintering. Porosities occur due to release of entrapped gases upon solidification. This is due to the large difference between the solidification temperatures of the constituent phases [1]. Porosities also arise in fabrication of FGMs using multi-step sequential infiltration technique. Porosities decrease the densities of the layers in FGM and reduces the stiffness. The small voids serve as stress concentrators in the layers. However, porous materials have key applications in engineering fields involving combustion synthesis, separation, and lightweight structures. Thus, the effects of porosities in complex systems under dynamic conditions such as an FG rotor-disc system must be taken into account during analysis. The present work aims to determine the vibration characteristics of an FG shaft system with porosities using three-dimensional finite element method.

A review of literature shows that several researchers have studied the vibration response of rotor systems composed of homogeneous isotropic materials. The effects of viscous and hysterical damping of a rotating shaft were presented in [2]. Including the effects of translational inertia and bending, a finite element model (FEM) for rotor system was developed by [3]. An evaluation of stability of a damped rotor system was presented by [4] by extending the linear finite element concepts. An important work by Nelson et al. [5] studied a method for dynamic modelling of rotor systems mounted with rigid discs, distributed parameter finite rotor elements and discrete bearings. Rotor-dynamics forms the backbone of the present study.

A variety of studies using FG materials are present in the literature. Chakraborty et al. [6], based on the theory of first-order shear deformation (FOSD), proposed a two-noded beam element for FGMs and applied it to static, thermal, and free vibrations problem. Free and forced vibration analysis of laminated FG beam under thermal-induced initial stresses was carried out by [7]. Reddy and Chin [8] studied the dynamic thermoelastic response of FG cylinders and plates using FEM and considering the effect of thermomechanical coupling in the formulation. Linear frequencies of simply supported FGM beams were presented in [9]. The vibration response of an FGM beam under different boundary conditions was presented by [10]. The study involved different beam theories for the analysis, [11] used a three-noded beam element based on Timoshenko beam theory to model a FG spinning shaft system and performed vibration and stability analysis. Another work [12] presented the free vibration analysis of a simply supported FG shaft system with transverse surface crack. A recent study [13] presents the three-dimensional finite element analysis of an FG shaft system to determine the vibration characteristics. However, the works reported in [6]-[13] are dealt with FG shafts and beams without porosity.

The dynamics of porous FG beams were evaluated by [1]. Linear and non-linear vibration analysis was carried out and the ends of FG beams were elastically restrained. Jahwari and Naguib [14] investigated FG porous plates modelled using different theories. The dynamics of an FG porous plate resting on foundations was studied by [15]. Using different beam

P. Sathujoda, Professor is with the Department of Mechanical and Aerospace Engineering, Bennett University, India (corresponding author, e-mail: prabhakar.sathujoda@bennett.edu.in).

A. Bose is with the Department of Mechanical and Aerospace Engineering, Bennett University, India (e-mail: arnab.bose@bennett.edu.in).

theories, [16] carried out the investigation to study dynamic of FG porous beams. Vibration characteristics of porous FG beams and different thermal loadings were examined by [17]. Akbas et al. [18] studied the thermal effects on vibration characteristics of FG deep beams with porosity effects. However, to the best of authors' knowledge, the dynamics analysis of a porous FG shaft system is rarely found in the literature. The objective of this study is to fill the research gap. The study involves three-dimensional FEM of an FG rotor-disc system with porosity using ANSYS commercial software. The shaft is supported on isotropic undamped bearings. Power law has been used for material gradation. The study attempts to formulate equations to model material property variation with porosity effects for FG shafts based on the works from literature involving FG porous beams. Whirl natural frequencies have been determined at different rotating speeds of the shaft. The effect of power law index and volume fraction of porosities on the whirl natural frequencies has been determined.

II. THEORY AND MATERIAL GRADATION LAWS

The material properties of FGMs are position and temperature dependent. The accurate gradation of material properties is achieved by varying the volume fraction of the constituents of FGM with respect to spatial coordinates. FGM structure consists of an outer ceramic rich region and inner metal rich region, and the gradation of materials occurs between these layers. To obtain a smooth variation of properties, the gradation is controlled using material laws. Researchers have reported several gradation schemes such as power law, exponential law, sigmoid law gradations and Mori-Tanaka scheme. However, power law is used in most applications. The position dependence of properties is obtained using the Voigt model, which gives a simple rule for the composite materials. The properties *(Pi)* unique to each layer are expressed using (1). *Pc* and *Pm* represents the material properties in ceramic rich and metal rich region. *Vc* and *Vm* stands for volume fraction of ceramic and metal, respectively.

$$Pi = PcVc + PmVm \qquad (1)$$

The summation of volume fractions of both constituents is unity, i.e. $Vc + Vm = 1$. The temperature dependence of material properties is achieved by (2), from the discussions in [19]. P0, P1, P2 and P3 are material dependent temperature coefficients available in [8].

$$P(T) = P_0 (P_{-1} T^{-1} + 1 + P_1 T^1 + P_2 T^2 + P_3 T^3) \qquad (2)$$

A. Power Law Gradation for Non-Porous FG Structures

For an FG shaft with circular cross-section, the gradation of material properties occurs in a radial direction. The inner core of the shaft is assumed to be of purely metal and the outer layer is purely ceramic. Fig. 1 represents the cut section view of solid FG shaft and Fig. 2 represents the radial layers of shaft cross section. For circular cross-sections the position and temperature dependent properties $P(r,T)$ are obtained using (3) [8].

$$P(r,T) = Pm(T) + \big(Pc(T) - Pm(T)\big)Vo(r),$$
$$Vo(r) = \left(\frac{r-Ri}{Ro-Ri}\right)^k, Ri \le r \le Ro, 0 \le k \le \infty \qquad (3)$$

Here, $Pm(T)$ and $Pc(T)$ refer to the material properties in metal and ceramic rich region respectively at temperature T (Kelvin). $Vo(r)$ refers to the volume fraction of metal phase at a radius r. Ri and Ro are the internal and external radius of the shaft. k is the power law coefficient.

The spatial and thermal dependent distribution of properties $P(z,T)$ of an FG beam having rectangular cross section (Fig. 3) is expressed using (4) [8]; where, h is the thickness and z is the thickness coordinate. $z = \frac{h}{2}$ at top surface and $z = \frac{-h}{2}$ at the bottom surface of the beam.

$$P(z,T) = Pm(T) + \big(Pc(T) - Pm(T)\big)Vo(z)$$
$$Vo(z) = \left(\frac{z}{h} + \frac{1}{2}\right)^k, \frac{-h}{2} \le z \le \frac{h}{2}, 0 \le k \le \infty \qquad (4)$$
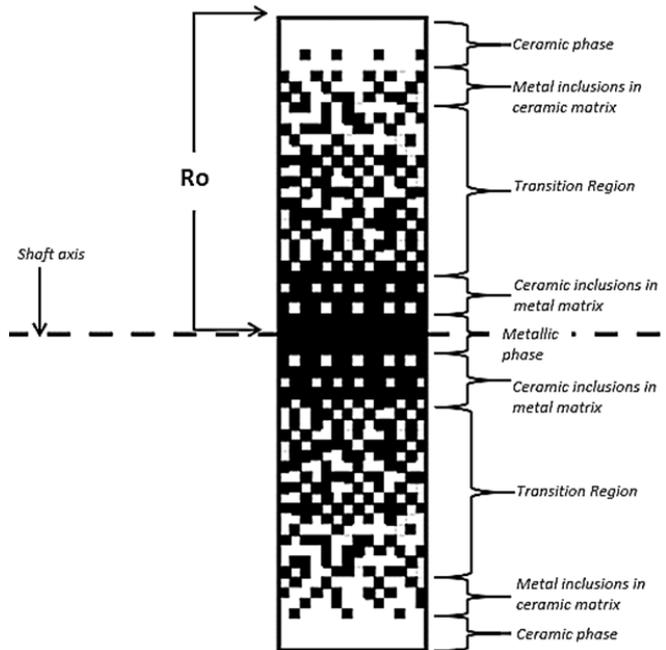

Fig. 1 Continuously graded microstructure in a cut section of the FG shaft

B. Power Law Gradation in Porous FG Structures

An even distribution of porosity along the radial direction is considered for analysis. Equation (4) depicts the layer wise porosity distribution along the cut section of a hollow shaft. Modified power law expressions of even porosities distribution for the FG shaft systems are proposed based on the power law expressions available for porous FG beams.
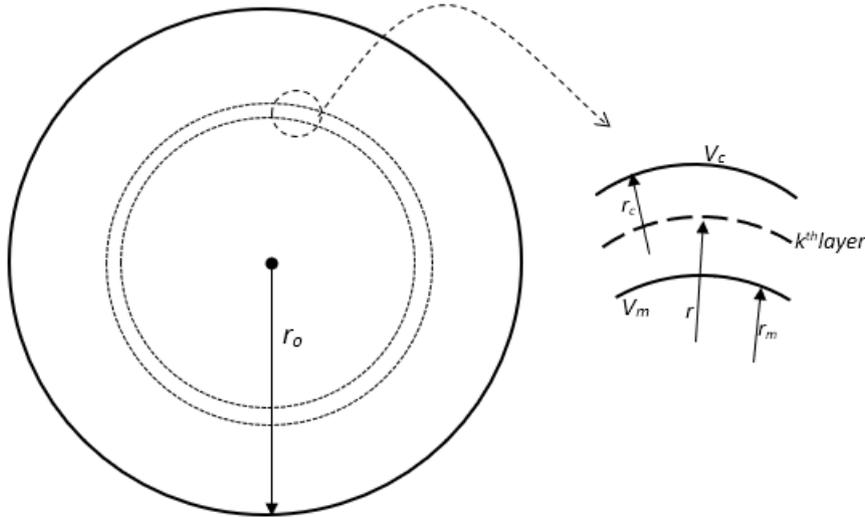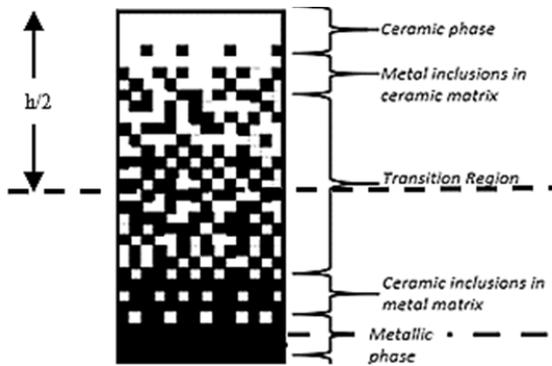
Fig. 2 Radial variation of volume fraction

Fig. 3 Continuously graded microstructure along rectangular cross-section of FG beam

The material properties distribution along a rectangular cross-section with even porosity variation is given as (5) [1]. All the symbols have the same meanings as discussed in (4). α is the volume fraction of porosities. If $\alpha = 0$ the FG beam becomes non-porous.

$$P(z,T,\alpha) = Pm(T) + \left(Pc(T) - Pm(T)\right)Vo(z) - \left(Pc(T) + Pm(T)\right)\frac{\alpha}{2}, \alpha \ll 1 \quad (5)$$

Based on (5), power law can be developed for porous FG shafts having circular cross section. Equation (6) represents the material property variation following power law for FG shaft with evenly distributed porosity.

$$P(r,T,\alpha) = Pm(T) + \left(Pc(T) - Pm(T)\right)\left(\frac{r-Ri}{Ro-Ri}\right)^k - \left(Pc(T) + Pm(T)\right)\frac{\alpha}{2}, \alpha \ll 1 \quad (6)$$

$$Ri \le r \le Ro, 0 \le k \le \infty, \alpha \ll 1$$

Equations (5) and (6) are used to determine Young's modulus, density, Poisson's ratio in each radial layer. Thermal conductivities are however assumed to be varied according to (4).

C. Temperature Gradation

For an axis-symmetric FG shaft with circular cross-section the heat conduction is given by (7).

$$\frac{d}{dr}\left[rK(r)\frac{dT}{dr}\right] = 0 \quad (7)$$

In absence of heat generation, (7) when subjected to the boundary conditions, $r = Ri$ at $T = Ti$ and $r = Ro$ at $T =$, yields the non-linear temperature distribution $T(r)$ given by (8) [19]. Here, $Km \wedge Kc$ refers to thermal conductivity of metal and ceramic respectively. Tm and Tc refer to the temperatures in metal and ceramic layer respectively. Also, $cm = Kc - Km$.

$$T(r) = Tm + (Tc - Tm)\left[\sum_{j=0}^{5}\left\{\frac{(-1)^j}{jk+1}\left(\frac{Kcm}{Km}\right)^j\left(\frac{r-Ri}{Ro-Ri}\right)^{jk+1}\right\}\right]\Big/\left[\sum_{j=0}^{5}\frac{(-1)^j}{jk+1}\left(\frac{Kcm}{Km}\right)^j\right] \quad (8)$$

D. Material Modelling in Present Work

The study involves modelling of a uniform steel disc mounted on an FG rotor system supported on isotropic bearings. The FG shaft is composed of Stainless Steel and Zirconia (SS-ZrO2). The inner metal core is made of SS and the outer layer the shaft is composed purely of ZrO2. The shaft is divided radially into 20 layers to model the gradation of material properties. The power law and the modified equations for porosity models govern the material properties. The material properties of the constituent materials used in the study are presented in Table I.

A Python code has been developed to generate the material property distribution in the layers of FG shaft and beam. Based on the cross-section (circular/rectangular), calculation

of the gradation of material properties is performed using Python code as discussed in the previous sections. An ANSYS macro is generated, which can be imported into the ANSYS model to apply the material properties. Fig. 5 shows the layer-wise material property variation along a typical FG shaft cross-section.

TABLE I
MATERIAL PROPERTIES AT ROOM TEMPERATURE

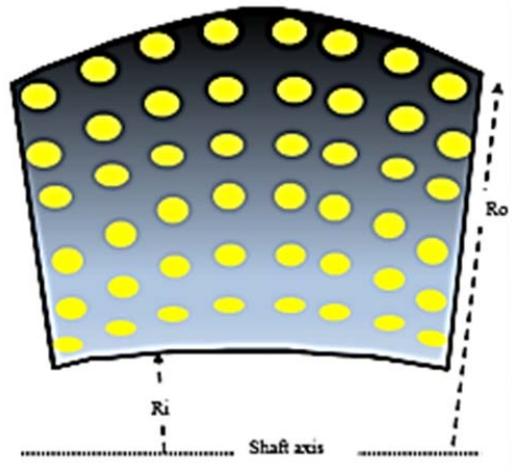| Property	Young's modulus (G Pa)	Density (kg/m^3)	Poisson's ratio
Steel	210	8166	0.3
Zirconia oxide	171.03	2370	0.24
Aluminum oxide	390	3960	0.26
Titanium	120	4420	0.31

Fig. 4 Even distribution of porosities along the radial direction in cut-section of an FG shaft
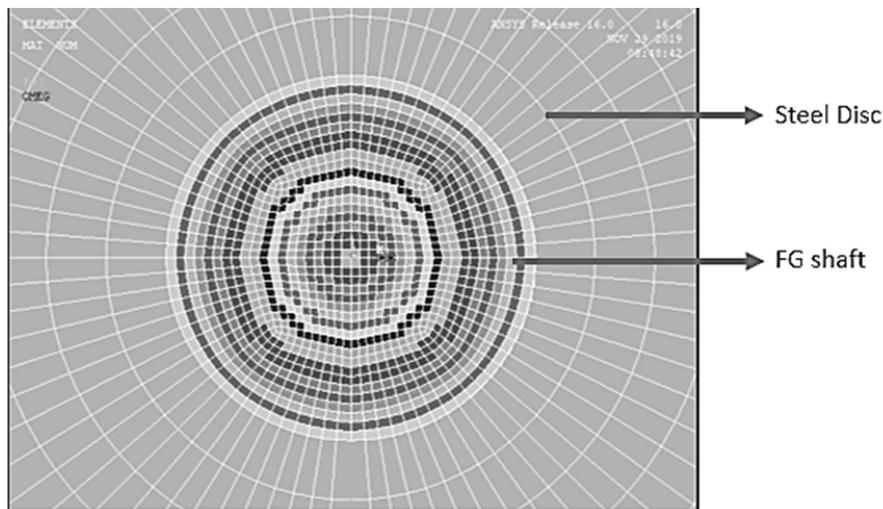

Fig. 5 Material gradation in SS-Al$_2$O$_3$ shaft modelled using ANSYS

III. GEOMETRY AND FE MODELLING

A. Rotor System Dimensions

The dimensions of the FG rotor system are based on the works by Shekhar et al. [20]. Fig. 6 shows the ANSYS model of the disc-rotor system. The radius and length of the solid shaft are 0.01 m and 0.5 m, respectively. The disc has a radius of 0.075 m, a thickness of 0.04 m and is located at the midspan of the shaft. The shaft is supported on isotropic bearings at both ends.

B. 3-D FEM

ANSYS commercial software has been used to carry out the three-dimensional FE modelling and analysis. Eight-noded SOLID-185 elements are used to model the FG shaft and steel disc. The element has three degrees of freedom at each node. The detailed element information can be found in ANSYS manual [21]. Map meshing is applied to the system and no warning elements or connectivity errors are reported.

Two-noded COMBIN-14 elements are used to model the bearing supports. The element has longitudinal spring damper characteristics. It is a uniaxial tension-compression element having three degrees of freedom at each node, translational along x, y, z directions. Two COMBIN-14 elements are attached to each shaft end. One end of a COMBIN-14 element is attached to the center of the shaft end, and the other end is fully fixed to the ground as shown in Fig. 6. The stiffness of the spring in both directions is taken as 1 MN/m. The bearing has no damping characteristics.

The shaft system has no internal damping and rotational velocity along the shaft axis is varied from zero to 4000 rpm.

IV. SOLUTION PROCEDURE

The equation of motion for the complete rotor-bearing system can be expressed as [4]:

$$M\ddot{p}(t) - G\dot{p}(t) + Kp(t) = f(t) \qquad (9)$$

The global mass matrix including the rotary and translational masses of the shaft is represented by M, the global gyroscopic matrix by G and K stands for global

stiffness matrix, including stiffness of the shaft and the bearing. $p(t)$ is the global nodal displacement vector, and f) is the global external force vector. External and gravity forces are neglected for the free vibration analysis.
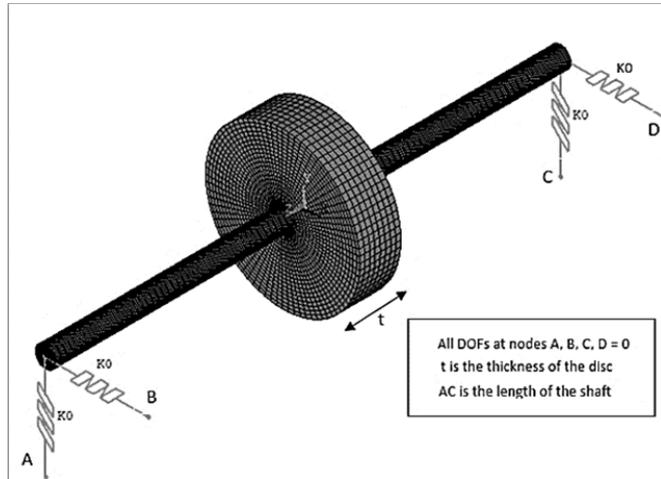

Fig. 6 ANSYS model of the double-disc shaft on bearing support

Block Lanczos solver scheme in ANSYS is used for vibration analysis for simply supported stationary FG shafts and beams discussed in the validation section. QR damped solver in ANSYS is selected to determine the whirl frequencies of FG rotor systems supported on bearings.

Equation (10) transforms the complete eigenvalue problem into modal subspace:

$$\{p(t)\} = [\phi]\{y\} \tag{10}$$

where, $[\Phi]$ refers to the normalized eigenvector matrix for the mass matrix $[M]$, and $\{y\}$ is the vector of modal coordinates.

Assuming no external forces, using the transformation for the differential equation of motion in modal subspace can be written as given in (11).

$$[I]\{\ddot{y}\} + [\phi]^T[C][\phi]\{\dot{y}\} + ([\Lambda^2] + [\phi]^T[Kunsym][\phi])\{y\} = \{0\} \tag{11}$$

where, $[\Lambda^2]$ is a diagonal matrix containing the first n eigenfrequencies ω_i [21].

V. VALIDATIONS

The literature review reveals that almost no significant work has been carried out involving porosities in FG shaft systems. Hence to verify the present work validations are performed at each stage to avoid discrepancies. Firstly, the material property distribution is validated with literature followed by the developed equation and code for porosity modelling. Natural frequencies of a simply supported FG shaft and a steel disc-rotor system have also been verified to validate the ANSYS model of the FG shaft system.

A. Material Property Distribution Verification

An FG shaft with inner core made of SS and Zirconium

Oxide outer layer is used to verify the layer wise material property distribution of the FG material used in present study. The shaft is non-porous and has a radius of 50 mm and length of 1.5 m. The inner core is kept at 300 K and outer ceramic at 900 K. The radial distribution of material properties such as Young's modulus and Poisson's ratio is presented in Figs. 7 and 8, respectively. The distribution profiles are in absolute confirmation with the graphs present in literature [22].
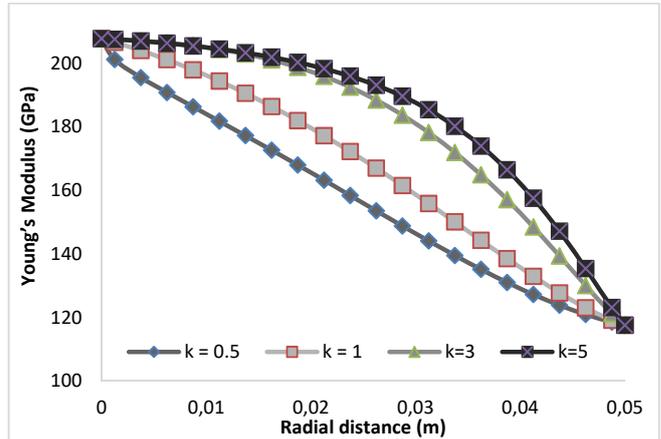

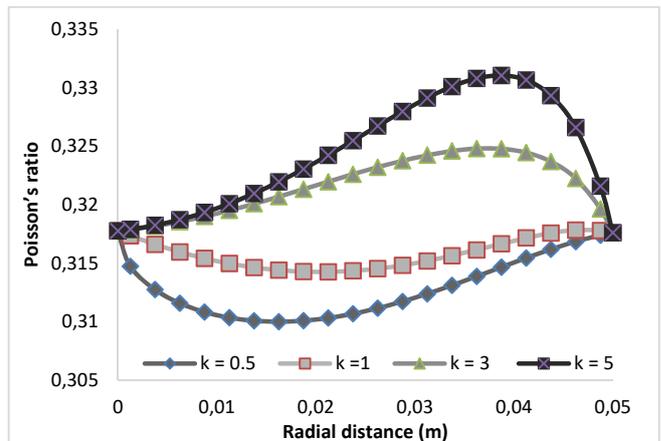Fig. 7 Radial variation of Young's modulus for a SS-ZrO2 FG shaft at Tm = 300 K and Tc = 900

Fig. 8 Radial variation of Poisson's ratio for a SS-ZrO2 FG shaft at TM = 300 K and Tc = 900

B. Verification of Developed Equations for Porous FG Shaft

Equation for the even porosity model are developed to radially distribute the porosities along the shaft cross-section. The presence of porosities reduces the densities in the layers. The density variation patterns in layers of (SS-ZrO2) FG shaft obtained using the developed equations. Fig. 9 compares the rate of variation of layer-wise densities of porous and non-porous FG shafts. Part a shows the density variation with radius for the FG shaft models and part b shows the difference in layer (ρ_{diff}) wise densities at same radial layer between non-porous and porous FG shaft. In a radial layer ρ_{diff} can be computed as:

$$\rho_{diff} \ = \ \rho_{porous} - \rho_{non-porous}.$$

The variations obtained are in conformation with the theoretical nature, which verifies the developed equations. The densities decrease in each layer because of increase in ceramic phase. However, the density difference remains constant in even porosity model as the voids and porosities are evenly distributed along the cross-section as shown in Fig. 4.

C. Validations Using Porous FG Beam

Due to absence of literature on porous FG shafts, FG beams with rectangular cross-section are selected to validate the porosity modelling using the Python program. The FG beam is modelled using Zirconium-Oxide at bottom and Titanium alloy at the top surface. The shaft is kept at a constant temperature of 300 K. The dimensions of the beam are kept same as in [17]. L/h ratio is kept a 20. The simply supported boundary conditions are obtained by fixing the two non-axial degrees of freedom for nodes on the two faces of the three-dimensional FE model of the beam a shown in Fig. 10. Non-dimensional frequencies ($\acute{\omega}$ are extracted for the porous FG beams models using (10). ω is the value of natural frequency,

E_m represents the Young's modulus of metal constituent in FG beam.

$$\acute{\omega} \ = \ \omega \frac{L^2}{h} \sqrt{\frac{\rho_m}{E_m}} \qquad (11)$$

The frequencies recorded show significant closeness to those found in [17] and are recorded in Table II. Frequencies have been obtained for even porosity models for $\alpha = 0, \alpha = 0.1, \alpha = 0.2$ and different power law coefficients. Thus, the porosity modelling method is extended further to porous FG shafts.

TABLE II
NON-DIMENSIONAL NATURAL FREQUENCIES FOR POROUS FG (TI - ZRO$_2$) BEAM

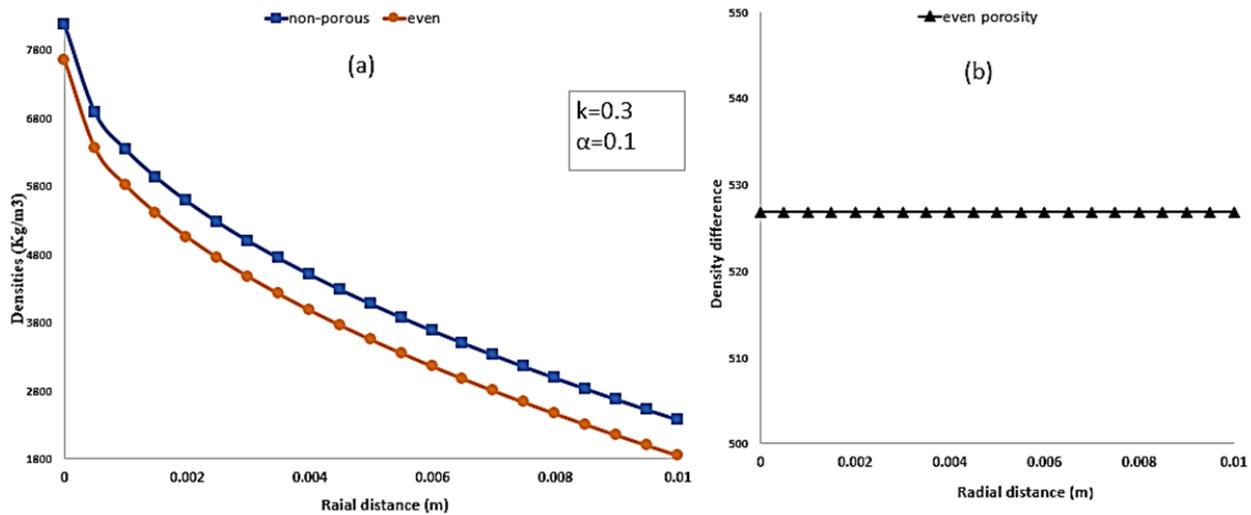| Porosity models	α	k = 0.5		k = 2	
		Present	Ebrahimi et al. [17]	Present	Ebrahimi et al. [17]
Even	0	4.527	4.515	3.566	3.55
	0.1	4.588	4.582	3.511	3.508
	0.2	4.676	4.667	3.455	3.449

Fig. 9 Density variation plots for SS-ZrO$_2$ FG shaft at room temperature. (a) Shows the radial density decrease and (b) shows the difference in densities between non-porous and porous (evenly distributed) FG shaft

D. Validation for a-Non-Porous FG Shaft

The material properties generated by the Python program have also been verified for non-porous FG shaft system for validation purpose. The shaft contains SS at the inner core and Al2O3 in the outermost layer. The shaft is kept at room temperature. The shaft is simply supported and Fig. 10 shows the side view of the shaft. The shaft has a radius of 40 mm and a length of 1 m. Power law coefficient (k) is kept as 0.5. The shaft has been divided into twenty layers radially to apply the gradation. Giving $\alpha = 0$ as input to the code yields material property distribution for a non-porous FG shaft. Finite element analysis of three- dimensional solid model of the shaft system is carried out to obtain the natural frequencies. The first and second natural frequencies are given in Table III and are

compared with the results from [11] for the FG shaft having the same dimensions as discussed, modelled using beam elements. The frequencies show a variation of only 0.027% and 1.4% variation, hence conforming the FG modelling technique used.

TABLE III
NATURAL FREQUENCIES (HZ) FOR SIMPLY SUPPORTED FG SHAFT

Modes	k = 0.5		
	Present	Gayen et al. [11]	Difference (%)
First	255.99	255.92	+0.027
Second	1003.5	1017.71	-1.4

E. Rotor-Disc FE Model Validation

Prior to extending the material modelling to FG rotor

system validations have been carried out for a steel disc mounted on homogenous shaft made of steel. The shaft-system has the same dimensions as shown in Fig. 6. The shaft system is supported on bearings at the ends. The stiffness and damping of the COMBIN-14 elements used to model the bearings is kept as 1.0E5 N/m and 100 Ns/m, respectively. Natural frequencies are determined for the three-dimensional solid FE model using ANSYS. First, two natural frequencies are compared with studies available in [20] and are listed in Table IV. The percentage difference between frequencies obtained in present work and those from literature is not significant, hence validating the FE rotor-disc system.

TABLE IV
NATURAL FREQUENCIES (HZ) FOR STEEL ROTOR-DISC SYSTEM

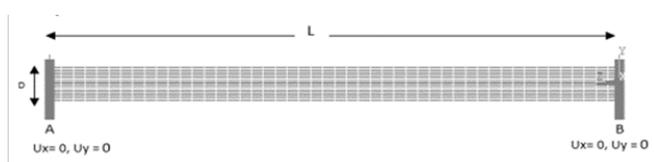| Modes	Steel Disc-Rotor System		
	Present	Sekhar and Prasad [20]	Difference (%)
First	24.2	24.27	+0.28
Second	94.5	95.2	+0.73

Fig. 10 Side view of a simply supported FG shaft/beam showing the boundary conditions

VI. RESULTS AND DISCUSSIONS

A. Effect of Power Law Coefficient

A single disc FG rotor bearing system, shown in Fig. 6 is composed of SS-ZrO$_2$, is considered to investigate the natural frequencies and whirl effects. Modelling has been achieved using power law. Even the porosity model is evaluated to model the micro-voids and porosities. The effect of material gradation on whirl frequencies has been studied. Campbell diagrams have been plotted to capture the backward and forward whirl frequencies. Attempts have been made to identify variation of fundamental frequencies with variation of power law coefficients and volume fraction of porosities. Suitable explanations are presented for the obtained variations in subsections below.

The even porosity model is used to understand the behavior of porosities in FG shafts. The shaft is kept at room temperature. Material properties are applied using the code validated in the previous section. Four different power law coefficients k from 0.5 to 5 are selected to study. Two porosity volume fractions are studied 0.1 and 0.2. Taking volume fraction of porosity as zero represents non-porous FG shaft condition. Variation of the first fundamental natural frequencies with porosity volume fraction coefficient at different power law coefficients is shown in Fig. 11.

The reasons for these variations can be attributed to the variation trends in Young's modulus of the shaft. Stiffness is directly related to the natural frequency thus the variation trends are governed by Young's modulus variation. The

averaged stiffness variation for an FG shaft k = 0.5 with two different α values is shown in Fig. 12. The first natural frequencies decrease with increase of power law coefficients. However, with increase in the value of porosity volume fraction, the fundamental frequencies show significant increase.
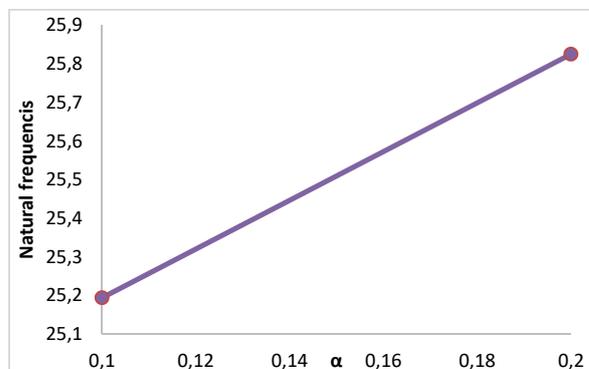

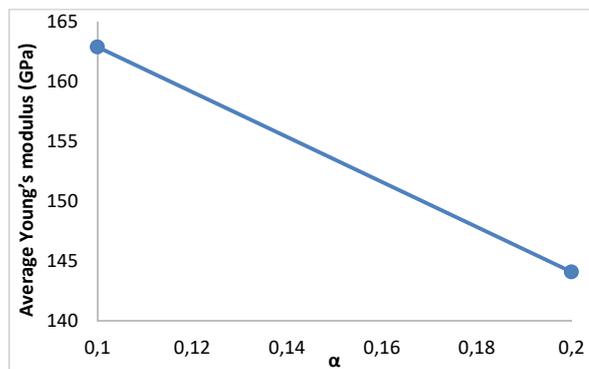Fig. 11 Natural frequency (Hz) for even porosity model

Fig. 12 Average Young's modulus variation for different porosity models

The general trend of decrease in natural frequencies with increase in the power law coefficient value occurs due to the reduction in stiffness at higher k values.

B. Effect of Porosity Volume Fraction (α)

The natural frequency variation trends for different volume fractions have been determined for the different porosity coefficients used. The plots of the trends obtained are presented in Fig. 13. The plot illustrates that for all k values the increase in porosity volume fraction increases the natural frequency of the system. The figure also shows that natural frequencies for the shaft system drop sharply till k = 1 and then decreases smoothly. The reasons for these trends are due to combined effect of Young's modulus variation in the FG shaft and mass of the shaft. The density variations discussed in earlier sections influence the weight of the shaft, which is inversely related to frequency of the shaft system.
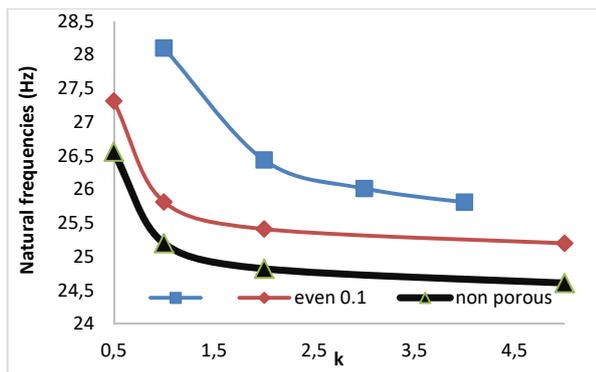
Fig. 13 First natural frequency variation for FG shaft with power law coefficient (k) modelled with different porosity coefficient values (α)

C. Whirl Frequencies for the FG Rotor-Disc System

The rotating speed of the shaft system is gradually varied to from stationary condition to 4000 rpm. The whirl frequencies at 0 rpm and 4000 rpm are recorded for few cases. As the speed is increased, the frequency occurring in pairs starts separating due to gyroscopic effects. The frequencies split to produce forward and backward whirls (FW & BW). The Campbell diagrams for the even porosity model studied for the FG shaft system, with k = 1 and α = 0, 0.1 and 0.2 are shown from Figs. 14-16.

The separation is also present in first FW and BW modes but is barely detectable on plots. However, the difference between the second FW and BW frequencies increases with increase of porosity volume fractions. This is because change in volume fraction of porosities affects the stiffness and densities of the FG shaft system which further effects the natural frequency variation.
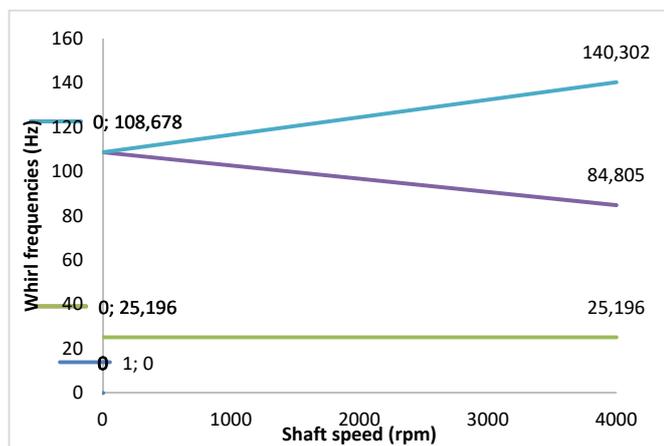

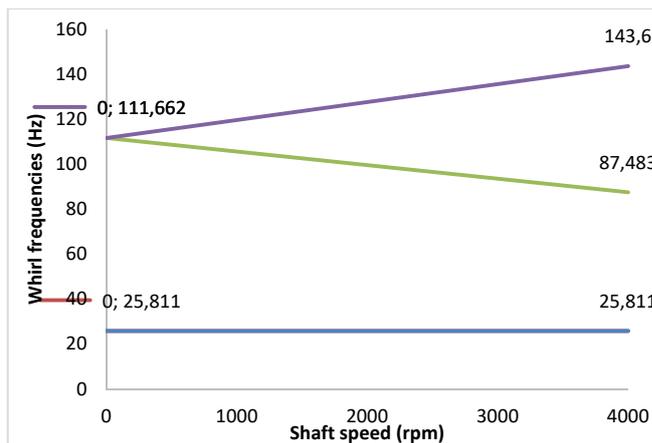Fig. 14 Whirl frequencies for FG shaft with no porosities (α = 0, k = 1)

Fig. 15 Whirl frequencies for FG shaft even porosities (α = 0.1)
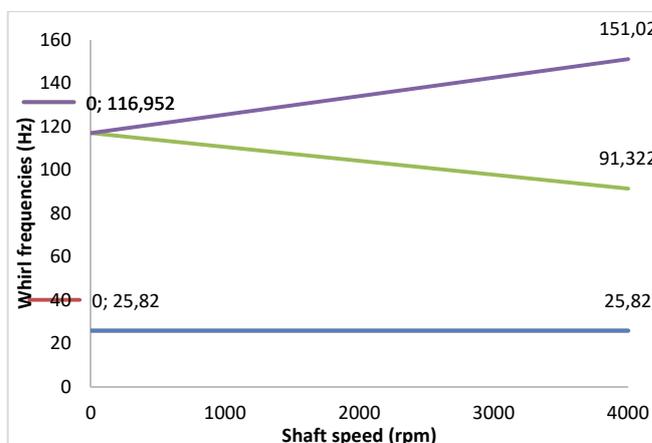

Fig. 16 Whirl frequencies for FG shaft even porosities (α = 0.2)

VII. CONCLUSIONS

Three-dimensional FEM and analysis of a porous FG disc-rotor system is carried out using ANSYS commercial software. SOLID 185 elements are used to model the shaft and disc. The shaft ends are supported on stiff isotropic bearings modelled using COMBIN 14 element. The FG haft has SS and Zirconium Oxide as its constituents and material property is governed by power law. The analysis has been carried out keeping shaft system at room temperature. The natural frequencies are extracted using ANSYS and the trends obtained are discussed. Notable conclusions from this study include the following:

- Development of equations and a Python program to generate the material property distribution based on power law for a porous FG shaft system. Even porosity distribution with different porosity volume fractions is studied.
- Natural frequencies of the shaft systems decrease with increase in power law coefficients for any porosity model due to reduction in stiffness.
- The natural frequencies of the FG shaft systems decrease with increase in power law index. This is due to increase in stiffness of the shaft.

- The natural frequencies increase with rise in the value of porosity volume fraction for any power law coefficient. The reasons for this behavior lie in the variation of Young's modulus and density variations.
- The whirl frequencies also decrease with increasing power law index. The frequencies increase with rise in porosity volume fraction. Also, it is observed that with increase in porosity volume fraction, the difference between the forward and backward whirls rises.

Future works in this direction would include the effects of thermal gradation on porous FG shafts and would aim to find more defining reasons for the trends and observations discussed in the present study.

REFERENCES

[1] Wattanasakulpong, N. and Ungbhakorn, V. (2014) "Linear and nonlinear vibration analysis of elastically restrained ends FGM beams with porosities," *Aerospace Science and Technology* 32(1), 111–120

[2] Dimentberg FM, Flexural vibrations of rotating shafts. London: Butterworths, 1961

[3] Ruhl R, Booker JF, A finite element model for distributed parameter turbo rotor systems. J Eng Ind 1972; 94: 128–132

[4] Nelson HD, Mcvaugh JM, The dynamics of rotor bearing systems using finite elements. J Eng Ind 1976; 98: 593–600

[5] Nelson HD, A finite rotating shaft element using Timoshenko beam theory. J Mech Des 1980; 102: 793–803

[6] Chakraborty A, Gopalakrishnan S, Reddy JN. A new beam finite element for the analysis of functionally graded materials. Int J Mech Sci 2003; 45: 519–539.

[7] Xiang HJ, Yang J. Free and forced vibration of a laminated FGM Timoshenko beam of variable thickness under heat conduction. Compos Part B: Eng 2008; 39: 292–303

[8] Reddy J.N., Chin C.D., 1998. Thermoelastical analysis of functionally graded cylinders and plates. J. Therm. Stresses. 21(6), 593-626

[9] Aydogdu, M. and Taskin, V. (2007) "Free vibration analysis of functionally graded beams with simply supported edges. "*Materials & Design* 28(5), 1651–1656.

[10] Simsek, M. and Aydın, M. (2017) "Size-dependent forced vibration of an imperfect functionally graded (FG) microplate with porosities subjected to a moving load using the modified couple stress Theory," *Composite Structures* 160, 408–421.

[11] Gayen D, Roy T (2014) Finite element based vibration analysis of functionally graded spinning shaft system. J Mech Eng Sci Part C 228(18):3306–3321

[12] Gayen, Chakraborty, Tiwari, Free Vibration Analysis of Functionally Graded Shaft System with a Surface Crack. Journal of Vibration Engineering & Technologies (2018) 6:483–494

[13] Arnab B, Prabhakar S, Natural frequency analysis of a functionally graded rotor system using the three-dimensional finite element method, Vibroengineering PROCEDIA,

[14] Jahwari, F. and Naguib, H. E. (2016) "Analysis and homogenization of functionally graded viscoelastic porous structures with a higher order plate theory and statistical based model of cellular distribution," *Applied Mathematical Modelling* 40(3), 2190–2205.

[15] Mechab, I., Mechab, B., Benaissa, S., Serier, B. and Bouiadjra, B. B. (2016b) "Free vibration analysis of FGM nanoplate with porosities resting on Winkler Pasternak elastic foundations based on two-variable refined plate theories," *Journal of the Brazilian Society of Mechanical Sciences and Engineering* 38, 2193–2211.

[16] Atmane, H. A., Tounsi, A., Bernard, F. and Mahmoud, S. R. (2015) "A computational shear displacement model for vibrational analysis of functionally graded beams with porosities," *Steel and Composite Structures* 19(2), 369–384.

[17] Ebrahimi, F. and Jafari, A. (2016) "A higher-order thermomechanical vibration analysis of temperature-dependent FGM beams with porosities," *Journal of Engineering* 2016

[18] Seref Doguscan Akbas, Thermal Effects on the Vibration of Functionally Graded Deep Beams with Porosity, International Journal of Applied Mechanics Vol. 9, No. 5 (2017) 1750076

[19] Touloukian YS. Thermophysical properties of high-temperature solid materials. New York: McMillan; 1967.

[20] Sekhar A.S., Prasad P.B. Dynamic analysis of a rotor system considering a slant crack in the shaft. Journal of Sound and Vibration (1997) 208(3), 457–474

[21] ANSYS Theory Manual

[22] Gayen D, Chakraborty D, Tiwari R, Whirl frequencies and critical speeds of a rotor-bearing system with a cracked functionally graded shaft – Finite element analysis, European Journal of Mechanics / A Solids (2016)